Supplement to “Stratospheric ozone trends and attribution over 1984-2020 using ordinary and regularised multivariate regression models”

Yajuan Li[1,2], Sandip S. Dhomse[3,4], Martyn P. Chipperfield[3,4], Wuhu Feng[3,5], Jianchun Bian[2,6,7], Yuan Xia[1] and Dong Guo[8]

1 School of Electronic Engineering, Nanjing Xiaozhuang University, Nanjing, China
2 Key Laboratory of Middle Atmosphere and Global Environment Observation, Institute of Atmospheric Physics, Chinese Academy of Sciences, Beijing, China
3 School of Earth and Environment, University of Leeds, Leeds, UK
4 National Centre for Earth Observation (NCEO), University of Leeds, Leeds, UK
5 National Centre for Atmospheric Science (NCAS), University of Leeds, Leeds, UK
6 College of Earth and Planetary Sciences, University of Chinese Academy of Sciences, Beijing, China
7 College of Atmospheric Sciences, Lanzhou University, Lanzhou, China
8 Key Laboratory of Meteorological Disaster, Ministry of Education/Joint International Research Laboratory of Climate and Environment Change/Collaborative Innovation Center on Forecast and Evaluation of Meteorological Disasters, Nanjing University of Information Science & Technology, Nanjing, China

Correspondence to: Yajuan Li (yajuanli@njxzc.edu.cn) and Sandip S. Dhomse (s.s.dhomse@leeds.ac.uk)

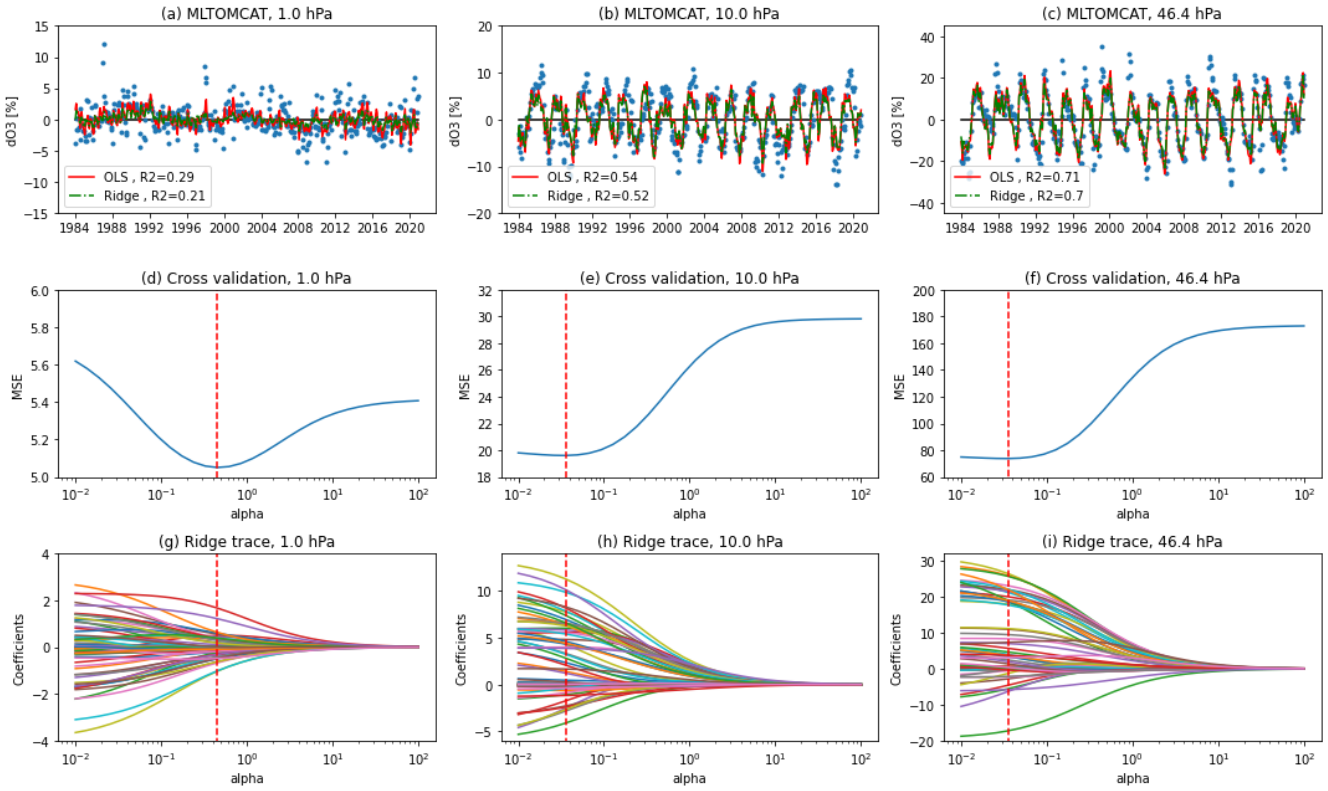

Figure S1: (a-c) Monthly ozone anomalies (blue dots) and the OLS (red line) and Ridge fitting (green dot-dashed line) from ML-TOMCAT data during 1984-2020 at the pressure levels of 1 hPa (left column), 10 hPa (middle column) and 46.4 hPa (right column) for the 1 °N latitude. (d-f) Cross-validated MSE values as well as (g-i) Ridge regression trace of the coefficients that change with alpha (α) are also shown. The vertical red dashed line indicates the optimal tuning value (α_0) for Ridge regression where the minimal MSE exists.

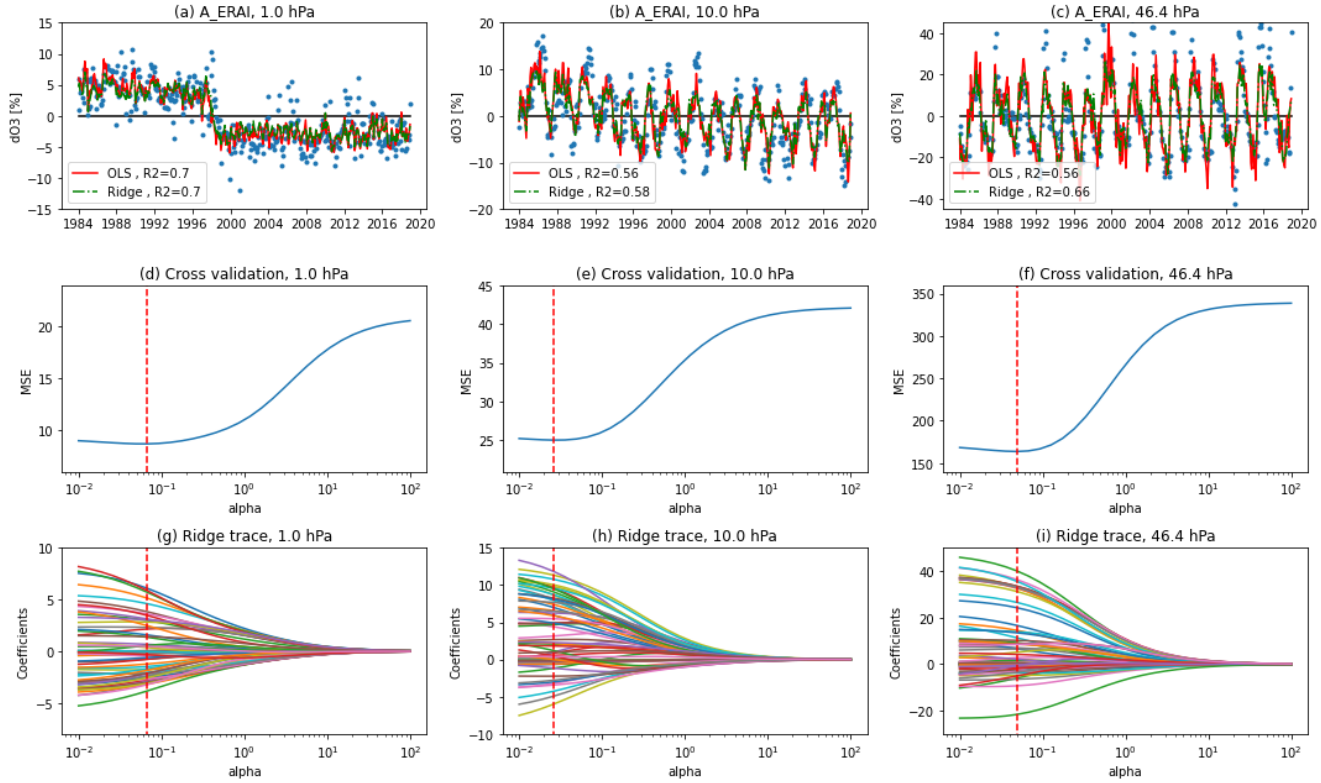

Figure S2: Same as Figure S1 but for simulation A_ERAI during 1984-2018.

30

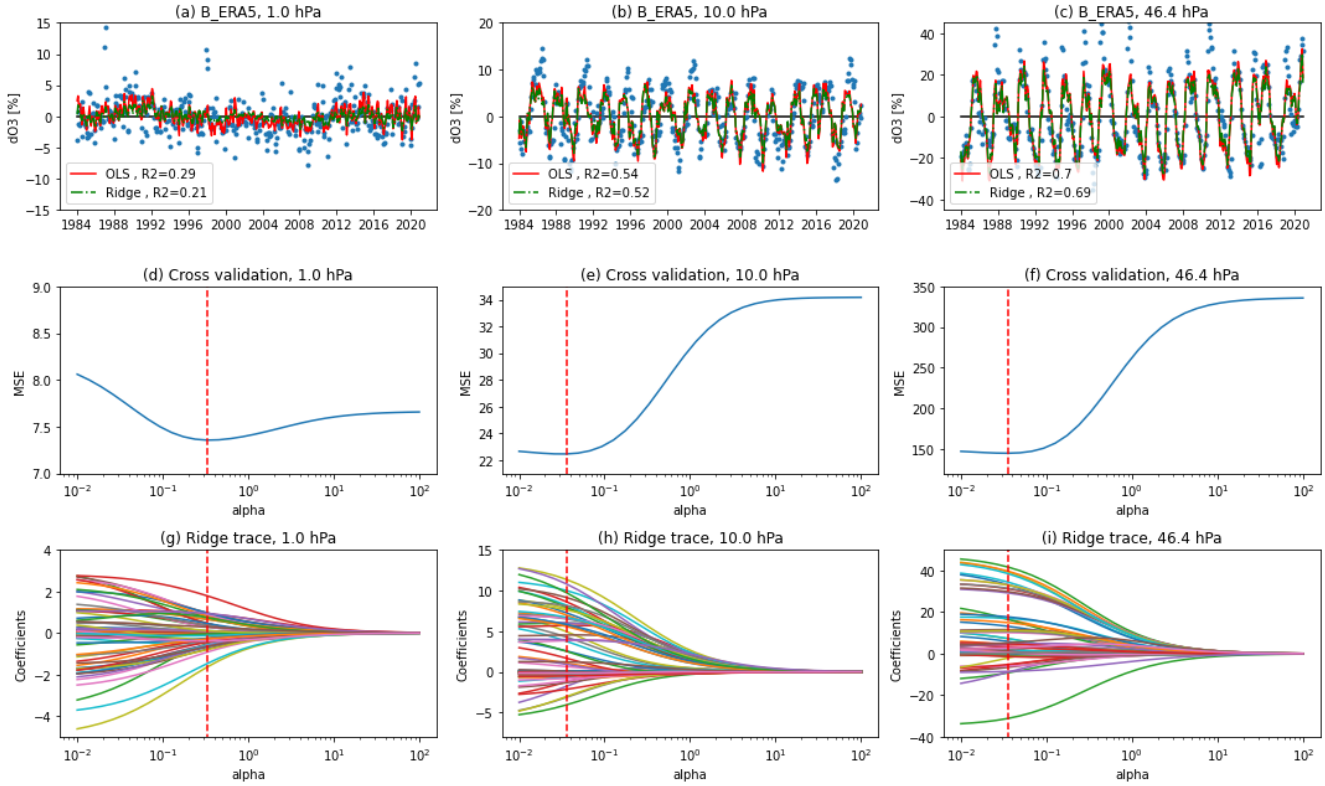

Figure S3: Same as Figure S1 but for simulation B_ERA5 during 1984-2020.

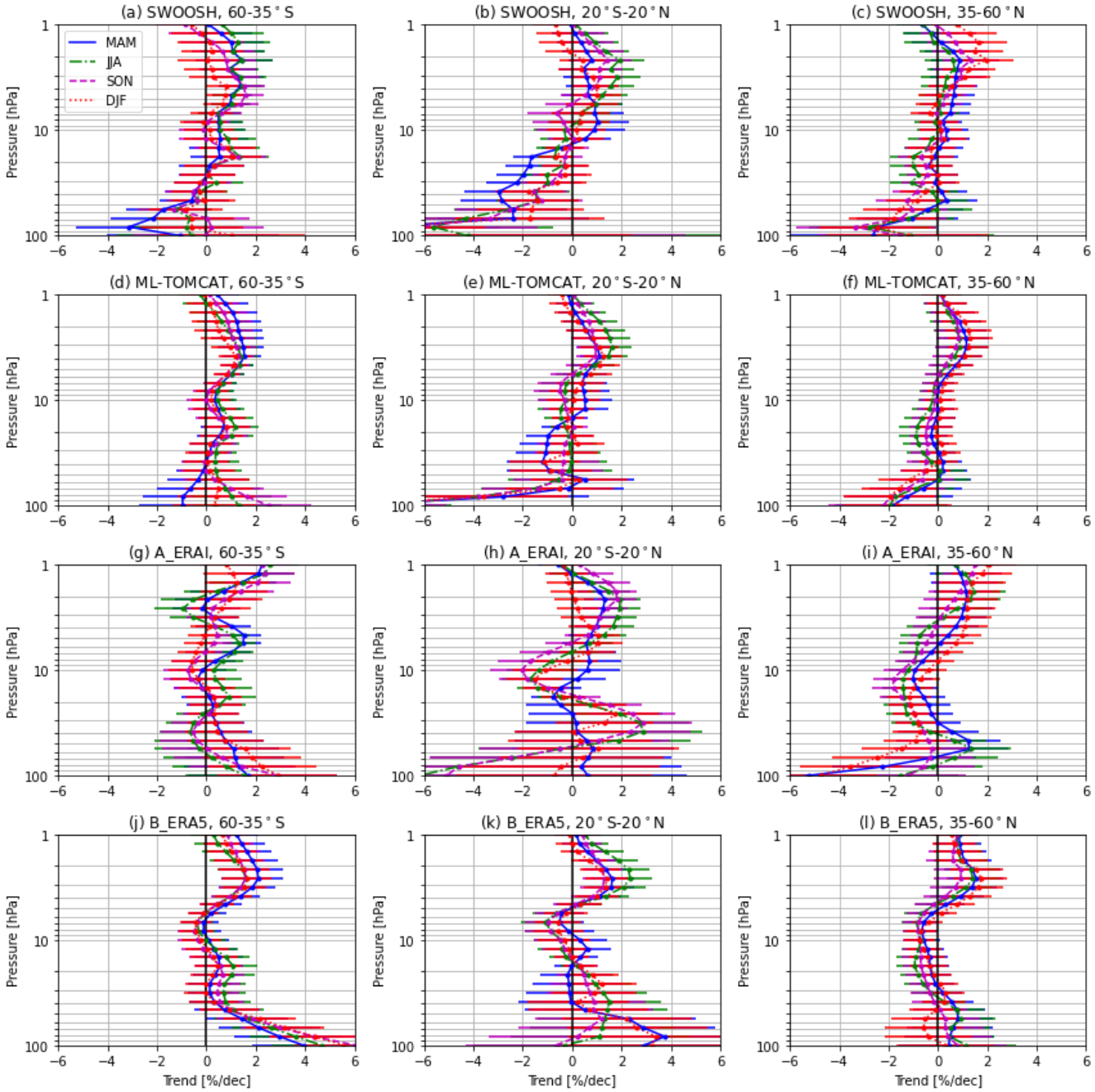

Figure S4: Profiles of seasonal ozone trends (blue for MAM, green for JJA, magenta for SON, and red for DJF) during post-1998 time periods from (a-c) SWOOSH, (d-f) ML-TOMCAT, simulation (g-i) A_ERAI and (j-l) B_ERA5 averaged over three latitude bands (60-35°S, 20°S-20°N, 35-60°N) based on the Ridge regression method. Error bars are 2-σ uncertainties.

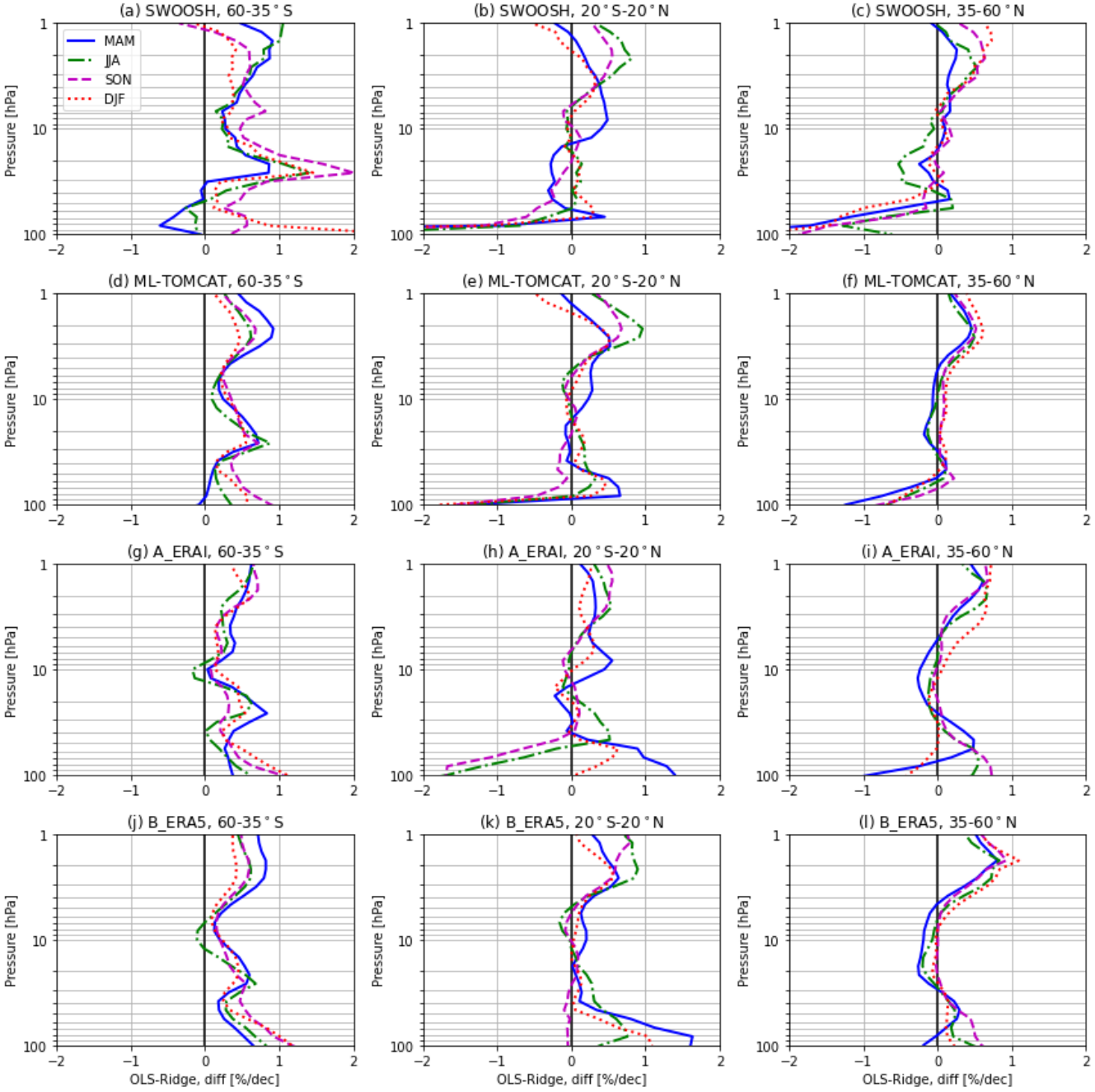

Figure S5: OLS-Ridge Differences of seasonal ozone trends (blue for MAM, green for JJA, magenta for SON, red for DJF) between OLS and Ridge regression methods averaged over three latitude bands (60-35°S, 20°S-20°N, 35-60°N) from (a-c) SWOOSH, (d-f) ML-TOMCAT, simulation (g-i) A_ERAI and (j-l) B_ERA5 during post-1998 time periods.

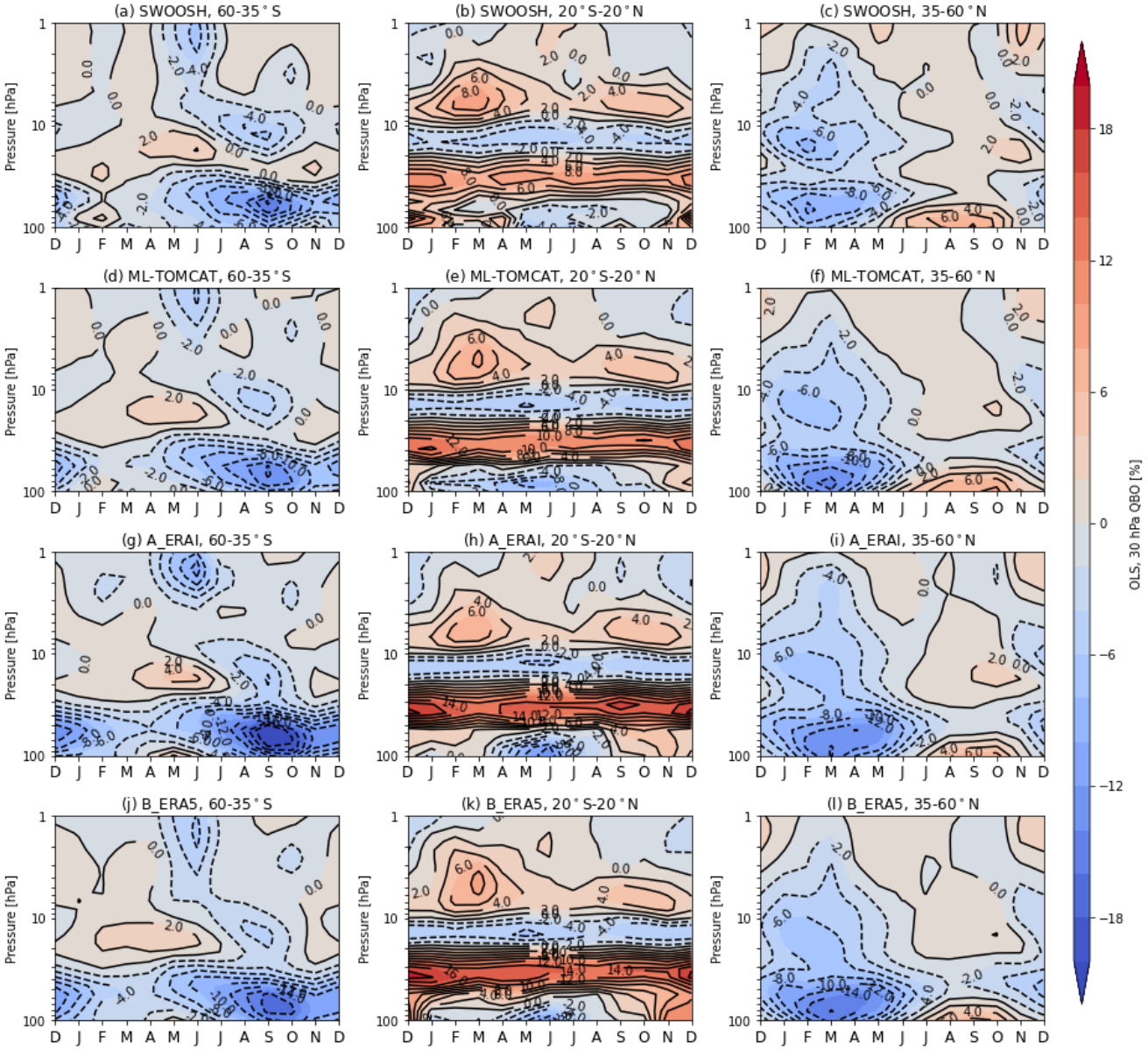

45 **Figure S6: Pressure-season variation of 30 hPa QBO in ozone (%) from (a-c) SWOOSH, (d-f) ML-TOMCAT, (g-i) A_ERAI and (j-l) B_ERA5 data for three selected latitudinal bands (60-35°S, 20° S-20°N, 35-60°N) based on the OLS regression method.**

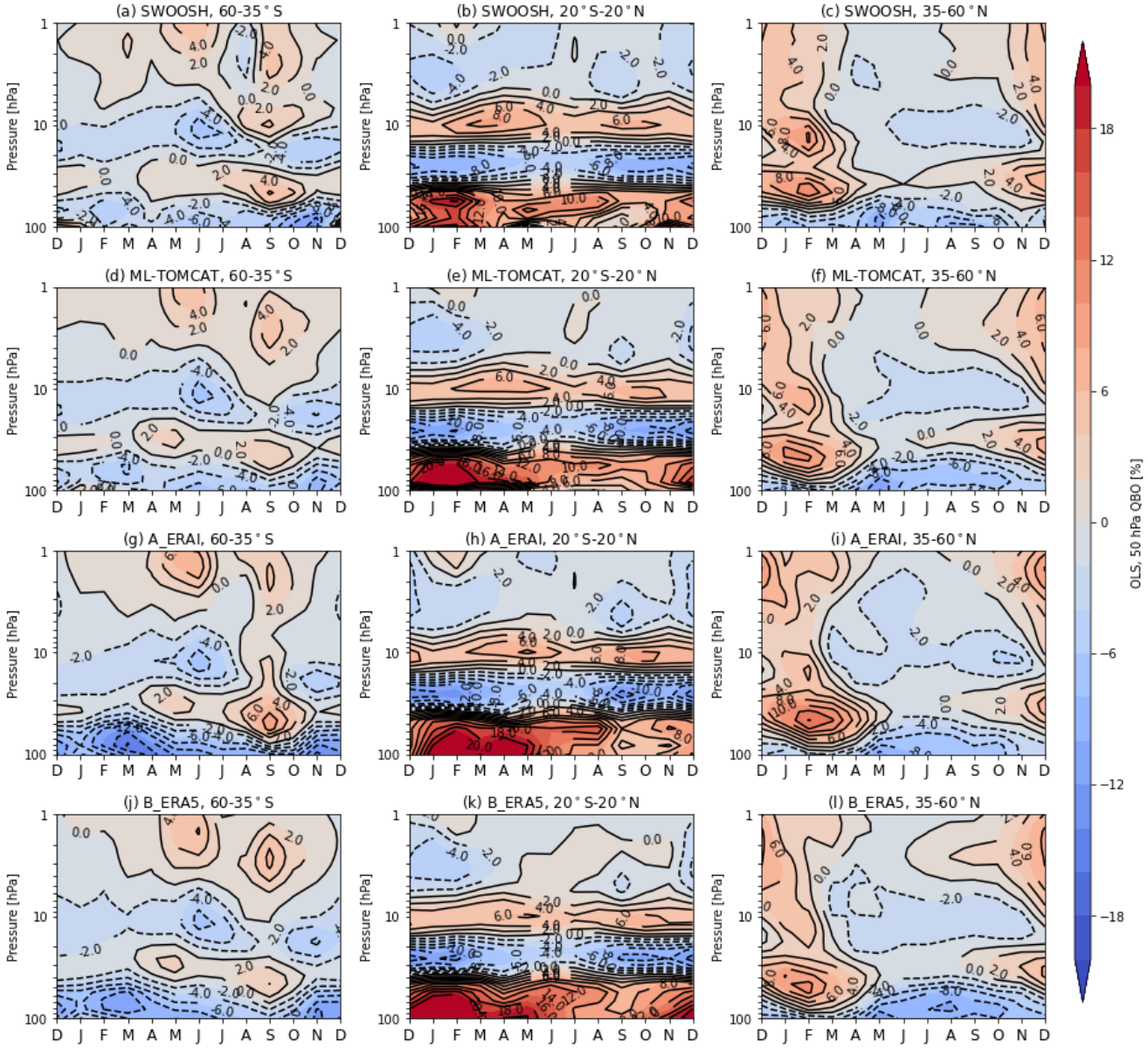

Figure S7: Same as Figure S6 but for 50 hPa QBO in ozone (%).

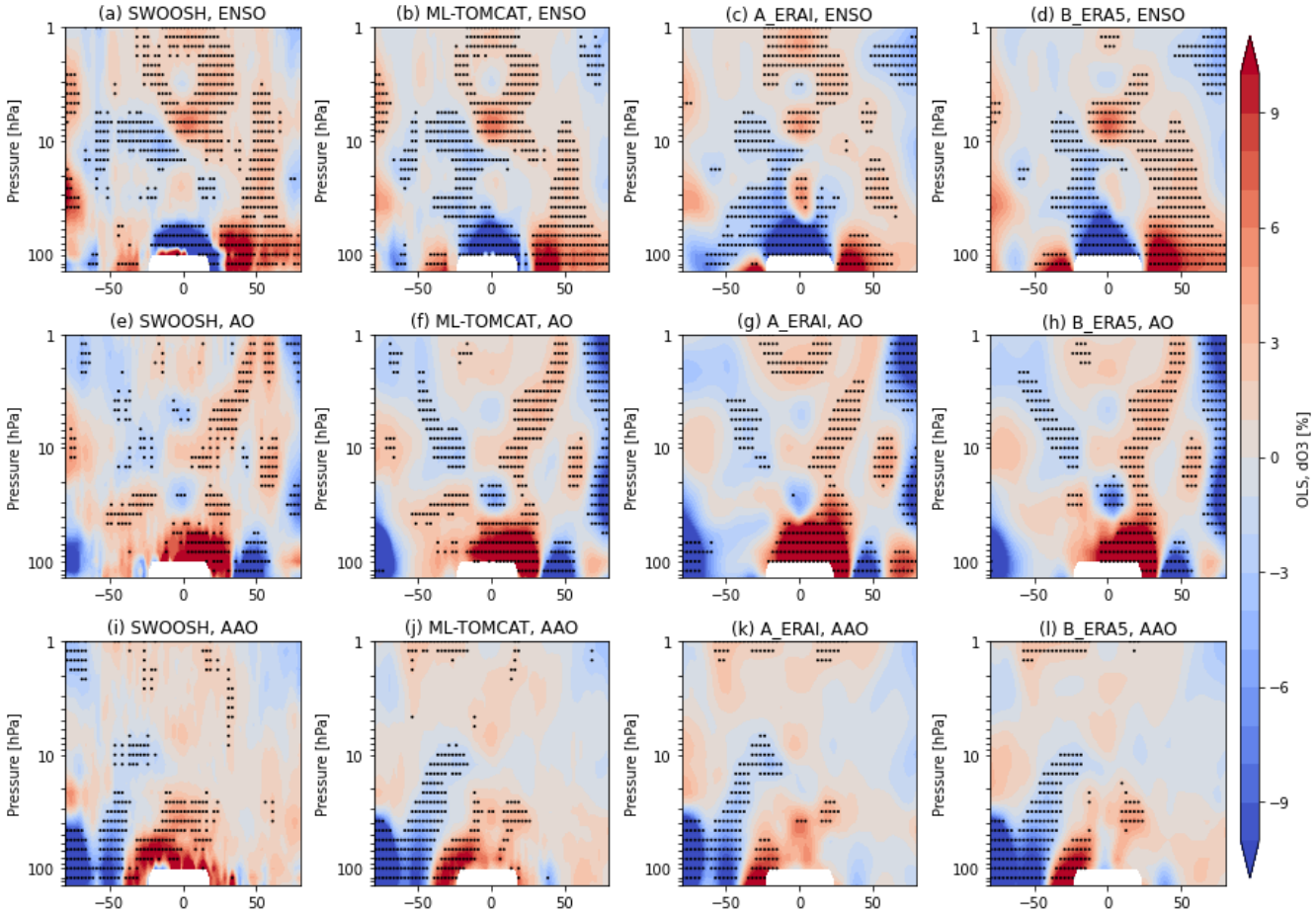

Figure S8: Pressure-latitude cross sections of the natural ozone variations (%) associated with (a-d) ENSO, (e-h) AO and (i-l) AAO derived from SWOOSH, ML-TOMCAT, and TOMCAT simulations (A_ERAI and B_ERA5) based on the OLS regression method. The stippling indicates regions that are significant at the 95 % level.